SLAC–PUB–7746
January 1998

Impedance and Wakefield in a Superconducting Beam Pipe*

F. Zimmermann
Stanford Linear Accelerator Center, Stanford University, California 94309

The impedance and the longitudinal wakefield in a superconducting beam pipe are derived. At low frequencies, this impedance is purely inductive, while at higher frequencies it approaches the resistive-wall impedance of a normal conductor. For very short bunches, the resistive heating of the beam pipe can induce quenches of the superconductor.

Submitted to Physical Review E

*Work supported by the U.S. Department of Energy under the Contract No. DE-AC03-76SF00515.

Impedance and Wakefield in a Superconducting Beam Pipe

Frank Zimmermann
Stanford Linear Accelerator Center
Stanford University, Stanford, California 94309

January 28, 1998

Abstract

The impedance and the longitudinal wakefield in a superconducting beam pipe are derived. At low frequencies, this impedance is purely inductive, while at higher frequencies it approaches the resistive-wall impedance of a normal conductor. For very short bunches, the resistive heating of the beam pipe can induce quenches of the superconductor.

1 Introduction

Recent years have seen a rapid progress in superconducting rf and accelerator technology at many laboratories around the world [1, 2, 3, 4, 5]. More ambitious projects are being proposed [6, 7]. Some of these projects consider operation with very short bunches, in which case their performance might be limited by short-range wakefields. In this report, we calculate the short-range wakefield and the impedance in a superconducting beam pipe and, in particular, we study the question if and how this wakefield differs from the resistive-wall wakefield in a conventional beam pipe. Based on the computed impedance, we then discuss under which circumstances the resistive energy loss could induce a quench, *i.e.*, a phase transition to the normal state.

The report is structured as follows. In Sections 2 and 3 we present formulae for the impedance, the wakefunction and the loss factor, which are derived from the BCS theory and applicable for type-I superconductors. These formulae involve integrals that must be evaluated numerically. In Section 4, we present approximate analytic expressions for the same set of quantities, considering the limiting cases of long and short bunches. Section 5 discusses the heating of the superconducting chamber wall due to resistive and geometric wakefields and the possibility of beam-induced quenches. In Section 6, we consider a few parameter examples, including the ultracompression option of the TESLA X-ray FEL design [6]. Finally, we draw some conclusions in Section 7.

2 Impedance

At low frequencies, the complex resistivity of a perfect superconductor is almost purely imaginary. As the frequency increases, the real part of the resistivity grows until, at a frequency comparable to the energy gap of the superconductor (divided by $\hbar$), it approaches the resistivity of the normal state. In general, the complex conductivity, $\sigma = \sigma_1 + i\sigma_2$, for arbitrary frequency and temperature can be obtained from the BCS theory [8]: In the limit that the field penetration depth is small compared with the superconducting coherence length ξ (this is fulfilled for type-I superconductors), the real and imaginary part of the conductivity are given by [9]

$$\begin{aligned}\sigma_1(\omega) &= \frac{2\sigma_n}{\hbar\omega}\int_{\epsilon_0}^{\infty}[f(E)-f(E+\hbar\omega)]\,g(E)\;dE + \\ &\quad \frac{\sigma_n}{\hbar\omega}\int_{\epsilon_0-\hbar\omega}^{-\epsilon_0}[1-2f(E+\hbar\omega)]g(E)\;dE \qquad (1)\\ \sigma_2(\omega) &= \frac{\sigma_n}{\hbar\omega}\int_{\epsilon_0-\hbar\omega,-\epsilon_0}^{\epsilon_0}\frac{[1-2f(E+\hbar\omega)](E^2+\epsilon_0^2+\hbar\omega E)}{(\epsilon_0^2-E^2)^{1/2}[(E+\hbar\omega)^2-\epsilon_0^2]^{1/2}}\;dE \qquad (2)\end{aligned}$$

where σ_n denotes the conductivity of the material in the normal state, $\epsilon_0(T)$ is the energy gap of the superconductor at temperature T (the energy required to break up a Cooper pair is $2\epsilon_0 \approx 3.52kT_c$), f is the usual Fermi-Dirac function,

$$f(E) = \frac{1}{e^{E/(kT)}+1}, \qquad (3)$$

and

$$g(E) = \frac{E^2+\epsilon_0^2+\hbar\omega E}{(E^2-\epsilon_0^2)^{1/2}[(E+\hbar\omega)^2-\epsilon_0^2]^{1/2}} \qquad (4)$$

The second term of Eq. (1) only appears if $\hbar\omega > 2\epsilon_0$, in which case the lower limit of (2) is $-\epsilon_0$ and not $\epsilon_0 - \hbar\omega$. The temperature dependence of the conductivity enters via the Fermi-Dirac function, $f(E)$, and also through the temperature dependence of the energy gap $\epsilon_0(T)$. For temperatures smaller than half the critical temperature, the energy gap is almost constant:

$$\epsilon_0(T) \approx \epsilon_0(0) \qquad \text{for} \qquad T < T_c/2 \qquad (5)$$

For simplicity we will henceforth ignore the weak temperature dependence of ϵ_0, although it would be straightforward to include. The complex conductivity, Eqs. (1) and (2), is illustrated in Fig. 1 for niobium ($\epsilon_0 \approx 1.4$ meV) at a temperature of 2 K.

At low temperatures and for sufficiently high frequencies, when the mean free path length of the metallic electrons becomes comparable to the classical skin depth, the surface resistance can acquire a finite value which is larger than the value expected from the classical skin depth and the bulk resistance. This phenomenon is called the 'anomalous skin effect' [10] and it is not included in

our further derivations. As a consequence, the formulae derived in this report could underestimate the actual wakefield in cases where the anomalous skin effect is important. Also not included in this paper is the ac component of the normal conductivity, often parametrized by a complex conductivity of the form $\bar{\sigma} = \sigma_n/(1 - i\omega\tau)$, with τ the relaxation time of the metal (typically $\tau \approx 10^{-14}$ s). The effect of the ac conductivity was investigated in Ref. [11]. It was found not to be very important, even for bunches as short as a few microns.

To compute the impedance of a superconducting beam pipe under the above assumptions and approximations, we now consider a point charge q moving from $s = -\infty$ to $s = +\infty$ at the speed of light in a round superconducting tube of radius b. Introducing the relative longitudinal position variable $z = -s+ct$, with negative values of z in front of the drive charge (s is the absolute longitudinal position, t the time at which the bunch center arrives at location s, and c the speed of light), the longitudinal impedance per unit length, Z, is related to the electric field by a Fourier transform,

$$Z(\omega) = -\frac{1}{qc}\int_{-\infty}^{\infty} dz\ E_s(z)e^{i\omega z/c}, \tag{6}$$

where the angular frequency ω can adopt positive and negative values.

The general form of the impedance can be obtained by solving Maxwell's equations with proper matching of the boundary conditions in the same way as for the conventional resistive-wall impedance; see, *e.g.*, Ref. [12]. The impedance is

$$Z(\omega) = \frac{2}{cb}\left[\left(\frac{\lambda c}{\omega} + \frac{\omega}{\lambda c}\right)\left(1 + \frac{i}{2\lambda b}\right) - \frac{i\omega b}{2c}\right]^{-1} \tag{7}$$

with

$$\lambda^2 = \frac{4\pi\sigma i\omega}{c^2} \tag{8}$$

and where the root of λ that is in the upper complex half plane must be chosen.

We can drop the very-low frequency term[1] $i/(2\lambda b)$ and the high-frequency term[2] $\omega/(c\lambda)$ [11, 12], and approximate Eq. (7) by

$$Z(\omega) = \frac{2}{cb}\left[\frac{\lambda c}{\omega} - \frac{i\omega b}{2c}\right]^{-1} \tag{9}$$

Equation (9) can be solved numerically, using the definition of λ, Eq. (8), and the conductivity predicted by the BCS theory, given in Eqs. (1) and (2). As an example, Fig. 2 shows the impedance described by Eq. (9), assuming[3] a realistic energy gap of $2\epsilon_0 \approx 0.15\ \hbar\omega_0$ and a temperature of 2 K. The difference between the 2-K and the 0-K conductivity is insignificant. Thus, all results presented in the following apply for niobium at any temperature between 0 K and 2 K. However, we note that at 5 Kelvin the real part of the low-frequency conductivity (shown by a dotted line) becomes non-negligible.

[1] The term $i/(2\lambda b)$ is negligible, if $f > c^2/(16\pi^2\sigma_n b^2) \approx 1$ Hz.

[2] This term is small at frequencies $f \ll 2\sigma_n \approx 10^{18}$–$10^{19}$ Hz.

[3] We will see in Section 6 that this is a realistic value for a niobium pipe of 3 cm radius.

In the treatment of resistive-wall wakefields, it is customary [11] to introduce the characteristic distance

$$s_0 \equiv \left(\frac{cb^2}{2\pi\sigma_n}\right)^{1/3}, \tag{10}$$

which depends on the beam-pipe radius and the conductivity (sometimes we also use the characteristic frequency $\omega_0 \equiv c/s_0$). In our case, it is natural to define a second distance, $\tilde{s}_g = c/\tilde{\omega}_g$, which is related to the critical temperature of the superconductor by $\tilde{\omega}_g \approx 6kT_c/\hbar$ [13].

For typical beam-pipe radii b and pure superconductors with a high normal conductivity σ_n, this second distance is always larger than the first one, *i.e.*, in most situations it is $\tilde{s}_g > s_0$. Now, depending on the size of the bunch length relative to s_0 and $\tilde{s}_g$, three cases can be distinguished: $\sigma_z < s_0 < \tilde{s}_g$ (case I), $s_0 < \sigma_z < \tilde{s}_g$ (case II), and $s_0 < \tilde{s}_g < \sigma_z$ (case III). In cases I and II, the bunch is shorter than the distance $\tilde{s}_g$, and, thus, the power spectrum extends beyond $\tilde{\omega}_g$. In these two cases, quenches due to resistive losses are most likely to occur. For larger bunch lengths (case III), the impedance experienced by the beam is mainly inductive. Although in this latter case there is no net energy loss, the inductive wakefield will give rise to an energy variation along the bunch, which might still affect the beam dynamics.

3 Wakefield and Loss Factor

The electric field excited by a point charge q (also called the *wakefunction*) is given by the inverse Fourier transform of the impedance,

$$\begin{aligned} E_s(z) &= -\frac{q}{2\pi}\int_{-\infty}^{\infty} d\omega\ Z(\omega)e^{-i\omega z/c} \\ &= -\frac{q}{\pi}\int_{-\infty}^{\infty} d\omega\ \ \mathrm{Re}Z(\omega)\cos(\omega z/c), \end{aligned} \tag{11}$$

and the wakefield for a real bunch distribution of total charge q is

$$E_{sb}(z) = \int_{-\infty}^{z} dz' E_s(z-z')\ \rho_z(z') = -\frac{q}{2\pi}\int_{-\infty}^{\infty} d\omega\ Z(\omega)\tilde{\rho}_z(\omega)e^{-i\omega z/c} \tag{12}$$

with ρ_z denoting the normalized charge distribution and $\tilde{\rho}_z$ its Fourier transform (for a Gaussian bunch of length σ_z it is $\rho_z(z) = \exp(-(z/\sigma_z)^2/2)$ and $\tilde{\rho}_z(\omega) = \exp(-(\omega\sigma_z/c)^2/2)$).

The energy loss due to the wakefield is given by $\Delta E/\Delta s = e^2N^2k_{tot}$, where e is the electron charge, N the bunch population (so that $q = Ne$), and k_{tot} the loss factor per unit length, for a Gaussian bunch defined by

$$k_{tot} = \frac{1}{\pi}\int_0^{\infty} d\omega\ \mathrm{Re}Z(\omega)\ e^{-(\omega\sigma_z/c)^2} \tag{13}$$

If the superconducting beam pipe is part of a cavity the resistive loss factor should be compared with the energy loss due to the geometric wakefield, which ultimately is also converted into heat by the residual resistivity of the superconducting beam pipe. Consider a cylidindrical cavity of length g, with a radius a, placed in a beam pipe of radius b. If $|b-a| \gg \frac{1}{2\pi}\sqrt{\lambda g/2}$ and $\sigma_z \ll b$ the loss factor per unit length for a single cavity follows from a diffraction model [14]:

$$k_{geom} \approx \frac{1}{\pi}\Gamma\left(\frac{1}{4}\right)\frac{1}{b}\frac{1}{\sqrt{\pi g \sigma_z}} \tag{14}$$

For a periodic array of many cavities the impedance per cavity is significantly smaller than the impedance of a single cavity at frequencies [15]

$$\omega \leq \frac{Mgc}{b^2}, \tag{15}$$

where M is the number of cavities. For the bunches we are considering, the dominant contributions to the loss factor and to the wakefield come from much higher frequencies. Consequently, in the following we ignore the interference between different superconducting cavities.

4 Simplified Expressions

In many cases, especially for very short and very long bunches, it is possible to bypass the complex expressions based on the exact BCS theory and instead to use a much simpler approximation, which often allows to derive explicit expressions for the quantities of interest. In the limits of very high and very low frequencies the complex conductivity of a superconductor is approximately given by [9, 13, 16]:

$$\sigma(\omega) \approx \begin{cases} i\ 2\sigma_n\tilde{\omega}_g/(\pi\omega) & \text{for} \quad \omega \ll \tilde{\omega}_g \\ \sigma_n & \text{for} \quad \omega \gg \tilde{\omega}_g \end{cases} \tag{16}$$

where the transition frequency $\tilde{\omega}_g$, introduced earlier, is roughly equal to $6kT_c/\hbar$. Here, T_c is the critical temperature of the superconductor, k Boltzmann's constant, and $\hbar$ Planck's constant. The energy $\hbar\tilde{\omega}_g$ is approximately twice the energy required to break up a Cooper pair.

Inserting Eq. (16) into Eq. (8) gives

$$\lambda = \begin{cases} i\sqrt{8\sigma_n\tilde{\omega}_g}/c & \text{for} \quad \omega \ll \tilde{\omega}_g \\ \sqrt{2\pi\sigma_n|\omega|}\ [i+\mathrm{sgn}(\omega)]/c & \text{for} \quad \omega \gg \tilde{\omega}_g \end{cases} \tag{17}$$

If we now use the expressions of Eq. (17) for the parameter λ in Eq. (9), we find that at low frequencies, *i.e.*, for $\omega \ll \tilde{\omega}_g$, the impedance is imaginary and the first term in the square brackets dominates, while at high frequencies ($\omega \gg \tilde{\omega}_g$) the impedance equals the well-known resistive-wall impedance of a

normal conductor [11]. Explicitly, in the two limits of very high and very low frequency, the impedance reads:

$$Z(\omega) \approx \begin{cases} -\frac{i}{b^2\omega_0}\left(\frac{\sqrt{\pi}\omega}{\sqrt{\omega_0\tilde{\omega}_g}}\right) & \text{for} \quad \omega \ll \tilde{\omega}_g \\ \frac{2}{b^2\omega_0}\left[\frac{2(1-i)+i(\omega/\omega_0)^{3/2}}{4(\omega_0/\omega)^{1/2}-2(\omega/\omega_0)+(\omega/\omega_0)^{5/2}/2}\right] & \text{for} \quad \omega \gg \tilde{\omega}_g, \end{cases} \tag{18}$$

For a long bunch ($\sigma_z \gg \tilde{s}_g$), we can integrate the formula for the wakefield, Eq. (12), using the inductive impedance of Eq. (18), and obtain

$$E_{sb}(z) = \frac{q s_0^{3/2} \tilde{s}_g^{1/2} z}{\sqrt{2} b^2 \sigma_z^3} \exp\left(-\frac{z^2}{2\sigma_z^2}\right). \tag{19}$$

Hence, the wakefield of a long bunch is proportional to the derivative of the charge distribution. This is different from the wakefield experienced by long bunches in a resistive pipe ($\sigma_z > s_0$), for which Piwinski [17] has derived the approximate expression

$$E_{rw}(z) = \frac{q}{4b^2}\left(\frac{s_0}{\sigma_z}\right)^{3/2} f(z/\sigma_z) \tag{20}$$

with $f(u) = |u|^{3/2} e^{-u^2/4}(I_{1/4} - I_{-3/4} \mp I_{-1/4} \pm I_{3/4})$, where the upper sign applies for $u < 0$, the lower sign for $u > 0$, and the argument of the modified Bessel functions I is $u^2/4$. The resistive wakefield, Eq. (20), is roughly proportional to the charge distribution itself.

In the opposite limit of short bunches ($\sigma_z < s_0$, $\sigma_z < \tilde{s}_g$), the superconducting wakefield approaches the short-range resistive wakefield of a normal conductor, which was calculated by Bane and Sands [11]. The energy loss in this limit is well approximated by [11]

$$k_{tot} \approx \frac{2}{b^2}\, e^{-3\sigma_z^2/s_0^2} \qquad (\sigma_z < s_0,\, \sigma_z < s_0) \tag{21}$$

This loss factor could be obtained from Eq. (13) by assuming an impedance equal to that of an undamped oscillator with resonant frequency $\omega_r = \sqrt{3}\, c/s_0$:

$$\text{Re}\; Z(\omega) \approx \frac{2\pi}{b^2}\, [\delta(\omega + \omega_r) + \delta(\omega - \omega_r)] \qquad (\sigma_z < s_0,\, \sigma_z < s_0) \tag{22}$$

5 Wall Heating

The resistive-wall energy losses raise the temperature of the beam pipe, which might result in quenches of the superconductor, *i.e.*, in overheating and transition to the normal state. We will estimate both the instantaneous heating of the beam-pipe surface during the passage of a single bunch and the quasi-stationary temperature increase for a long beam pulse consisting of many bunches.

First, let us consider the passage of a single bunch. The energy loss per unit length is

$$\frac{dE}{ds} = k_{tot} e^2 N^2 = m_e c^2 k_{tot} r_e N^2, \tag{23}$$

where N denotes the bunch population. We can write the energy deposition per bunch and per unit beam-pipe area as

$$\tilde{Q} \equiv \frac{dE}{2\pi b\ ds} = \frac{k_{tot} e^2 N^2}{2\pi b}. \tag{24}$$

The loss factor k_{tot} can be obtained either by numerically integrating Eq. (13), or, in case of a short bunch, also by using the approximate solution, Eq. (21). For short bunches (case I), the quasi-instantaneous temperature rise is given by

$$\Delta T = \frac{\tilde{Q}}{c_p \rho\ \delta_p(\omega_r)} \tag{25}$$

where c_p denotes the specific heat, ρ the density, and $\delta_p(\omega_r)$ the penetration depth of the electromagnetic field at the frequency $\omega_r = \sqrt{3}\ \omega_0$, and where we have assumed the simplified resonator impedance of Eq. (22). Ignoring the possibility of the anomalous skin effect, we take $\delta_p(\omega_r)$ as equal to the classical skin depth at the resonant frequency ω_r: $\delta_p(\omega_r) \approx c/\sqrt{2\pi\omega_r\sigma}$.

If we do not consider a smooth pipe but a cavity, we can calculate the energy deposition due to the additional geometric wakefields by replacing k_{tot} in Eq. (24) with the geometric loss factor k_{geom} of Eq. (14), which is valid if $\sigma_z < b$. Assuming that the diffracted power is ultimately absorbed by the finite resistivity of the superconductor and that it is not removed by higher-order mode dampers or by some other means, Eq. (25) can be used, also in case of geometric wakefields, to obtain a reasonable estimate for the induced temperature rise[4].

Second, we can estimate the quasi-stationary temperature rise for a long bunch train. We consider a train of n_b bunches uniformly distributed over the pulse time t_p. The average power deposited per unit area of the beam pipe is

$$P = \frac{n_b \tilde{Q}}{t_p}. \tag{26}$$

If the train is long, a steady state with increased temperature may be established during the train passage. We expect this to occur when the transverse spread of the heat wave at the end of the train, $x(t_p) \approx \sqrt{k(T)\ t_p / c_p \rho}$ (where $k(T)$ is the thermal conductivity at temperature T), is larger than the thickness d of the beam-pipe wall. The steady-state temperature increase on the inside of the beam pipe is then

$$\Delta T \approx \frac{Pd}{k(T)}, \tag{27}$$

where P denotes the deposited power, Eq. (26), and we have assumed that the outer side of the beam pipe is held at the constant temperature T.

[4] In this case, we suggest to replace, in Eq. (25), the skin depth at the resonant frequency ω_r, $\delta_p(\omega_r)$, by the skin depth at the characteristic bunch frequency, $\delta_p(c/\sigma_z)$.

6 Example

As an illustrative example, we consider a beam pipe made from pure superconducting niobium. We assume a residual resistivity ratio RRR[5] equal to 500 [6], so that the normal conductivity at 2 K is about $\sigma_n \approx 3 \times 10^{19}$ s^{-1}. Some further properties of niobium are listed in Table 1, which also gives the equivalent parameters for room-temperature copper.

Figure 3 shows the longitudinal electric field, Eq. (11), that is generated by a point charge of charge q in a niobium pipe of radius $b = 3$ cm. The solid line refers to superconducting, the dash-dotted line to normal conducting niobium. The difference between the two curves is very small, suggesting that the superconductivity hardly affects the wake for short bunches. Also shown as a dotted line is the wakefunction for a normalconducting copper beam pipe at room temperature. The difference between copper and niobium is due to the 50 times higher normal conductivity of the pure niobium (at low temperature) and not due to its superconductivity.

Figure 4 displays the wakefield for a Gaussian charge distribution considering several ratios σ_z/s_0. The electric field on the vertical axis is scaled by $(\sigma_z/s_0)^{3/2}$. Inspection of Eq. (20) shows that, for a normal conductor, this scaling would result in a universal wakefield shape in the limit of long-bunch lengths [11]. A drawback is that, by scaling in this way, we are hiding the strong increase of the wakefield with shorter bunch length. Figure 4 demonstrates that, in the case of short bunches with identical σ_z/s_0 ratios, the wakefields for copper and niobium as well as those for superconducting and normal-conducting niobium are very similar, if scaled according to Eq. (20). Thus, indeed, for short bunches there is no difference in the wakefield between a normal and a superconducting beam pipe. However, as the bunch gets longer and its rms length becomes comparable to the characteristic length $\tilde{s}_g$ of the superconductor ($\sigma_z \geq \tilde{s}_g \approx 38$ μm or $\sigma_z/s_0 \geq 4$), the wakefields in the normal and superconducting cases start to differ markedly. In accordance with expectation, both for a normal-conducting niobium pipe and for a copper pipe the wakefield of a long bunch, $\sigma_z/s_0 = 5$, is resistive and roughly proportional to the charge distribution, whereas the superconducting wake is mainly inductive and approximately proportional to the derivative of the distribution.

Next, in Fig. 5, we show the loss factor for a Gaussian bunch, obtained by numerically integrating Eq. (13). The approximation Eq. (21), describing the short-bunch limit, is also depicted. For $\sigma_z < s_0$, it describes the exact loss factor quite well.

The loss factor allows us to estimate the heat load on the vacuum-chamber wall and the resulting temperature rise. Let us consider, as an example, beam parameters as produced in the ultracompression option for the proposed X-ray laser facility at TESLA [6]. In this proposal, the bunch train transported through the superconducting TESLA linac is 1 ms long ($t_p = 1$ ms), and contains $n_b = 11000$ bunches, with a bunch population of $N = 6 \times 10^9$. The final rms

[5] RRR is defined as the ratio of resistivities at room temperature and at 10 K (just above T_c) [6].

bunch length, after ultracompression, is about 2 μm[6]. According to either Fig. 5 or Eq. (21), the loss factor in a smooth pipe for bunches of this length is $k_{tot} \approx 2/b^2$. Taking b as equal to the iris radius in the TESLA superconducting cavities (about 3 cm), Eq. (24) yields the power deposited per unit area of the beam pipe due to the nonzero resistivity: $\tilde{Q} \approx 10^{-4}$ J m^{-2}. Again assuming a niobium beam pipe at 2 K, with a skin depth at $\omega_r \approx 4 \times 10^{13}$ s^{-1} of about 3 nm, Eq. (25) predicts a surface temperature rise[7] of up to $\Delta T \approx 35$ K!

For a superconducting cavity, we can calculate the energy deposition due to the geometric wakefields by inserting into Eq. (24) the loss factor k_{geom} of Eq. (14). This loss factor is also depicted in Fig. 5, by the dash-dotted line. Using a length g equal to the TESLA cell period of 115.4 mm, the power deposited per unit area of the chamber surface is approximately $\tilde{Q}_{geom} \approx 2 \times 10^{-3}$ J m^{-2}. Thus, the energy deposition in the cavity is about 20 times larger than the energy deposition in a smooth pipe whose radius equals the cavity iris radius. For a skin depth δ_p of about 2 nm (evaluated at $\omega \approx c/\sigma_z$) and assuming the entire radiated energy is rapidly absorbed by the finite resistivity of the superconductor[8], the expected temperature rise according to Eq. (25) [9] is enormous, about 1000 K.

Whether a large temperature rise of a thin surface layer can cause a quench or whether, alternatively, the temperature change only constitutes a short-lived fluctuation remains to be studied and will likely depend on details of the cooling and vacuum system. Also a Cooper-pair recombination time short compared with the bunch length could prevent the development of a quench [18]. Unfortunately, such recombination times are not well known or, at least, not well documented. Despite these uncertainties, the magnitude of the estimated temperature rises indicates that the energy loss caused by the geometric and resistive short-range wakefields could be a potential limitation for some future applications.

Finally, let us estimate the steady-state temperature rise over the entire bunch train. The average power deposition per unit area, Eq. (26), is 1000 Wm^{-2} for a smooth pipe, and 20000 Wm^{-2} for a cavity. Assuming a thermal conductivity of $k(T) \approx 0.3$ W cm^{-1} K^{-1} and a wall thickness of $d = 0.5$ mm (which is equal to the outward spread $x(t_p)$ of the heat wave after the 1-ms pulse time) the average temperature rise, Eq. (27), is about $\Delta T \approx 0.04$ K, for the smooth pipe, which appears negligible, but as large as 1 K for the cavity, which would constitute a significant heat load. If the beam-pipe radius is reduced to 1 cm, the temperature rise during the bunch-train passage would increase to 1 K for the smooth pipe and to 9 K for the cavity! If the bunch length is increased from 2 μm to 25 μm, corresponding to the bunch length prior to the final ultracompression in the TESLA FEL design, the temperature change of

[6]The present TESLA design [6] does not envision bunches this long to traverse any superconducting cavity, but the last superconducting cavities are located before the final compression stage, where the bunches still have an rms length of 25 μm.

[7]This is an overestimate, since the specific heat is not a constant but increases strongly with temperature.

[8]Here 'rapidly' means on a time scale shorter than the time for thermal relaxation over the distance δ_p.

[9]This is clearly an overestimate, as stated before.

the smooth pipe would be 30 times smaller, and the cavity temperature change would be reduced by about a factor of 5.

7 Conclusion

At low frequencies, the impedance of a superconducting beam pipe is inductive, which leads to an approximately linear energy variation along the bunch, but yields no net energy loss. At frequencies higher than the energy gap of the superconductor, the impedance becomes resistive and approaches the value of the normal state. As a result, the wakefield for short bunches is nearly equal to that generated in a normal conducting pipe at the same temperature. Even so, since, for typical pure superconductors, the normal conductivity at low temperatures is very high, the wakefields are smaller than they would be for a copper beam pipe at room temperature.

If operation with ultra-short bunches is planned, care has to be taken to avoid quenches (*i.e.*, transitions to the normal state) caused by the resistive-wall energy loss. The estimated instantaneous temperature increase for a 2-μm long bunch passing through a beam pipe of 3 cm radius is several centigrades, and it increases dramatically if also geometric wakefields must be absorbed. Details of the cryogenics design will decide if this sudden local temperature increase gives rise to a beam-induced quench or not. While the instantaneous heating from a short bunch can be large, the average temperature increase during the passage of a multi-bunch train is unlikely to exceed 1 degree Kelvin for a smooth beam pipe. However, for a cavity or an array of cavities, the average temperature increase during a long beam pulse can be several centigrades, unless the energy radiated at the geometric transitions is absorbed by a special material or coupled out of the cavity.

The wakefield effects considered in this paper are likely to impose a lower bound on the inner radius of superconducting beam pipes and rf structures in some future accelerators, in particular those operating with very short bunches.

Acknowledgements

I am very grateful to Rainer Wanzenberg from DESY, who first mentioned to me the possibility that the field of very short bunches can break up Cooper pairs, thus stimulating my interest in this problem, and who also pointed me to Ref. [16]. I also want to thank Karl Bane, Reinhard Brinkmann, Peter Schmüser and David Whittum for various helpful discussions. This work was supported by the US Department of Energy under Contract No. DE–AC03–76SF00515.

References

[1] R. Sundelin et al., "Superconducting cavity beam test in CESR", IEEE Trans. Nucl. Sci. 30, p. 3336 (1983).

[2] B. Dwersteg et al., "Beam test of a 9 cell superconducting cavity in the PETRA storage ring", IEEE Trans. Nucl. Sci. 32, p. 3596-3598 (1985).

[3] K. Kubo et al., "Four years of operation of the TRISTAN superconducting rf system", Proc. of HEACC92, vol. 2, p. 691, International Journal of Modern Physics A, Proceedings Supplements (1992).

[4] C. Reece et al., "Performance and installation status of superconducting cavities at CEBAF", Proc. of HEACC92, vol. 2, p. 951, International Journal of Modern Physics A, Proceedings Supplements (1992).

[5] SL RF group, "Experience with superconducting rf cavities in LEP", Part. Accel. 54, p. 15–24 (1996).

[6] R. Brinkmann, G. Materlik, J. Rossbach, A. Wagner (eds.), et al., "Conceptual Design of a 500 GeV e+e- Collider with Integrated X-Ray Laser Facility", in particular, Chapter 5, "A Super-Brilliant X-ray Laser Facility", DESY 97-048 (1997).

[7] R. Corsini, A. Hofmann, "Consideration on a FEL based on LEP superconducting cavities", CERN-SL-96-07-AP (1996).

[8] J. Bardeen, L.N. Cooper and J.R. Schrieffer, Theory of Superconductivity, Phys. Rev. 108, 1175 (1957).

[9] D.C. Mattis and J. Bardeen, 'Theory of Anomalous Skin Effect in Normal and Superconducting Metals', Phys. Rev. Vol. 111, no. 2 p. 412 (1958).

[10] G. Reuter and E. Sondheimer, Proc. Roy. Soc. A195, p. 336 (1949).

[11] K. Bane and M. Sands, 'The Short-Range Resistive Wall Wakefields', Proc. of Micro Bunches Workshop, Upton, New York, AIP Conference Proceedings 367, p. 131 (1995)

[12] A. Chao, Physics of Collective Beam Instabilities in High Energy Accelerators, John Wiley & Sons, New York (1993).

[13] M. Tinkham, Superconductivity, Gordon and Breach, New York, London, Paris, 1st edition 1965, and 2nd edition 1996.

[14] Reference [12], Equation (2.142).

[15] S.A. Heifets and S.A. Kheifets, "Coupling Impedance in Modern Accelerators", Rev. Mod. Phys., Vol. 63, no. 3 (1991).

[16] D.M. Ginsberg and M. Tinkham, 'Far Infrared Transmission through Superconducting Films', Phys. Rev. Vol. 118, no. 4 p. 990 (1960).

[17] A. Piwinski, DESY Report 72/72 (1972).

[18] R. Brinkmann, private communication (1997).

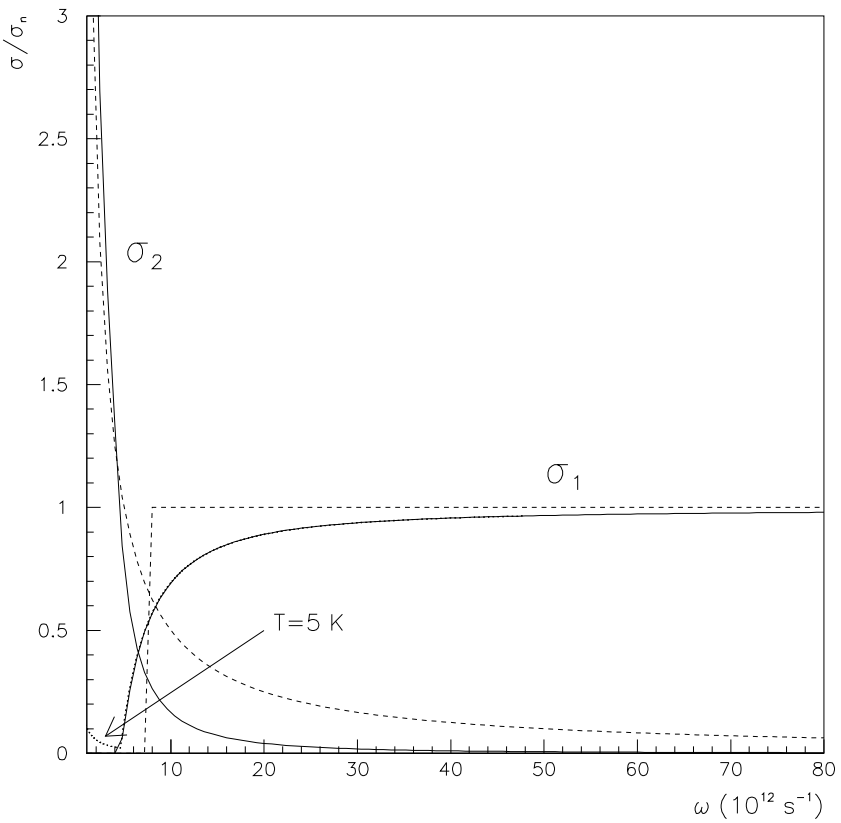

Figure 1: Complex conductivity, according to Eqs. (1) and (2), for niobium at a temperature of 2 K, as a function of the angular frequency. The vertical axis is normalized to the conductivity of the normal state, σ_n. The horizontal coordinate is given in units of inverse picoseconds. The dotted line in the left lower corner is the real part of the conductivity for a temperature of 5 K. The dashed lines represent the approximation of Eq. (16).

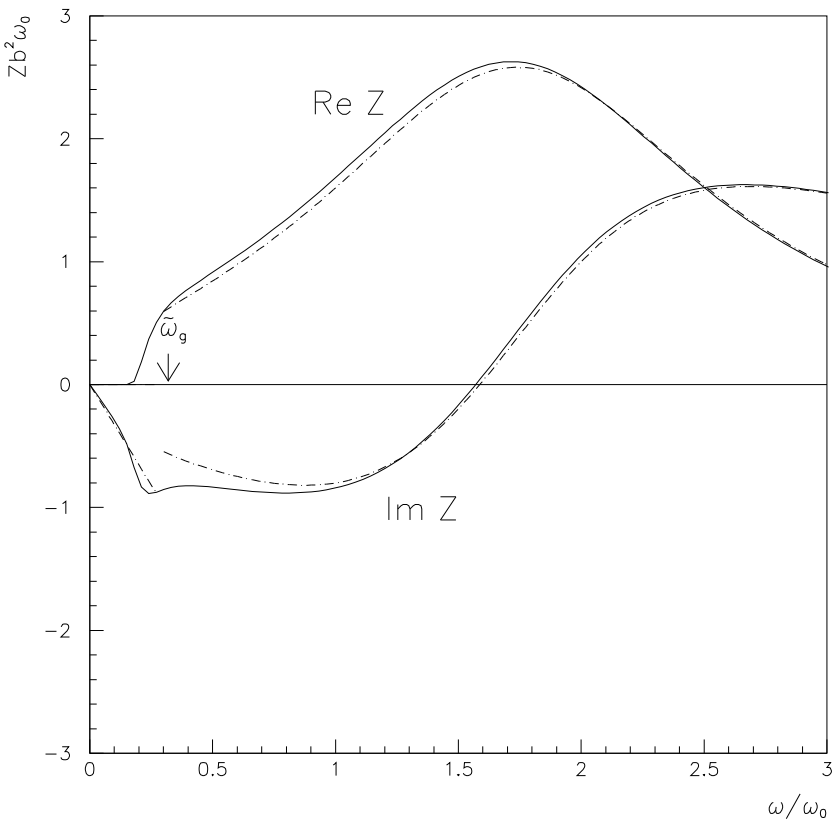

Figure 2: Longitudinal impedance, according to Eq. (9), for a niobium pipe ($\sigma_n \approx 3 \times 10^{19}$ s^{-1}, $T_c \approx 9.5$ K) with 3 cm radius at a temperature of 2 K as a function of the angular frequency ω. The frequency $\tilde{\omega}_g$ is indicated by an arrow. The horizontal axis is normalized to ω_0. The vertical axis gives the impedance in units of $1/(b^2\omega_0)$, where ω_0 denotes the characteristic distance $(cb^2/(2\pi\sigma_n))^{1/3}$ of Eq. (10). The dashed lines represent the approximations of Eq. (18).

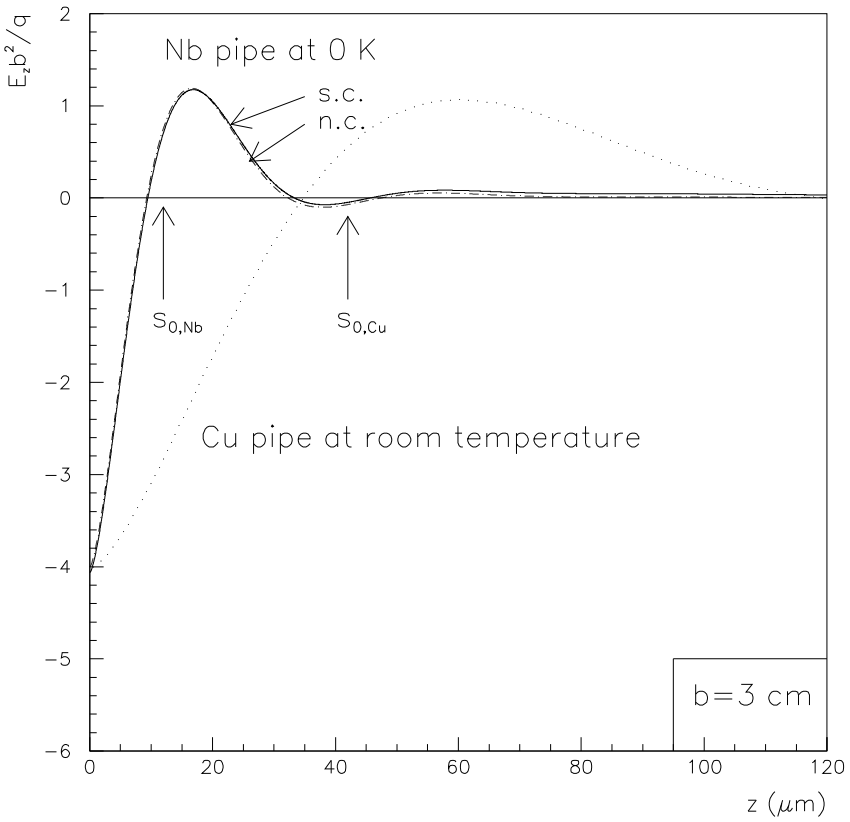

Figure 3: Longitudinal wakefield $E_z b^2/q$ left behind by a point charge of charge q in a beam pipe of radius b, calculated according to Eqs. (11), (9), (8), (2) and (1), for a s.c. niobium tube at 2 K (solid curve); the wakefield for a normal-conducting niobium pipe with otherwise identical parameters (dash-dotted); and the short-range resistive-wall wakefield for a copper pipe at room temperature (dotted). The characteristic distances s_0 for niobium and copper are indicated by the vertical arrows.

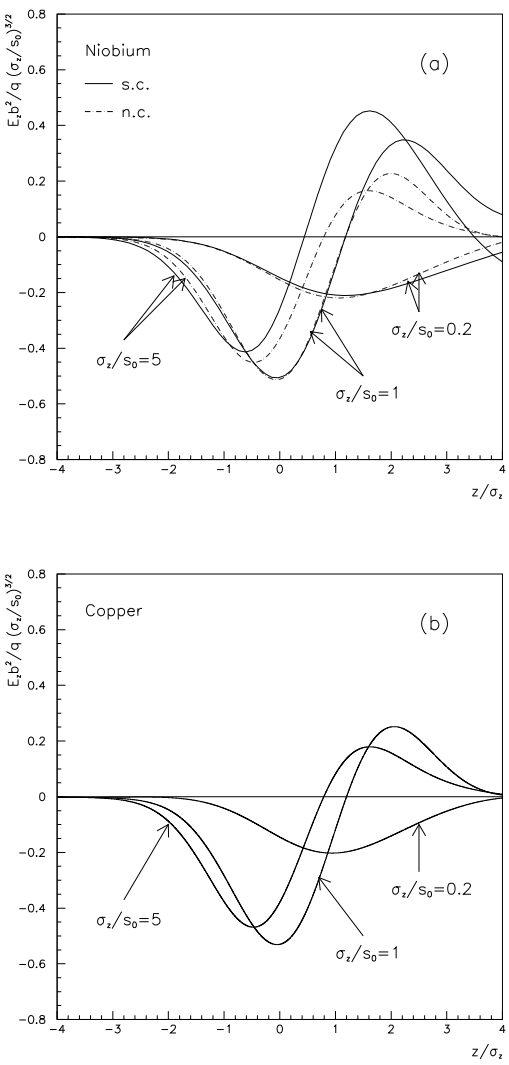

Figure 4: Longitudinal wakefield $E_z b^2/q$ of a Gaussian bunch of charge q in a beam pipe of radius b for several values of σ_z/s_0, according to Eqs. (12), (9) (8), (1) and (2); (a) for a s.c. niobium beam pipe at 2 K; (b) for a copper beam pipe at room temperature. The dash-dotted curve in figure (a) shows, for comparison, the wakefield of a normal-conducting niobium beam pipe.

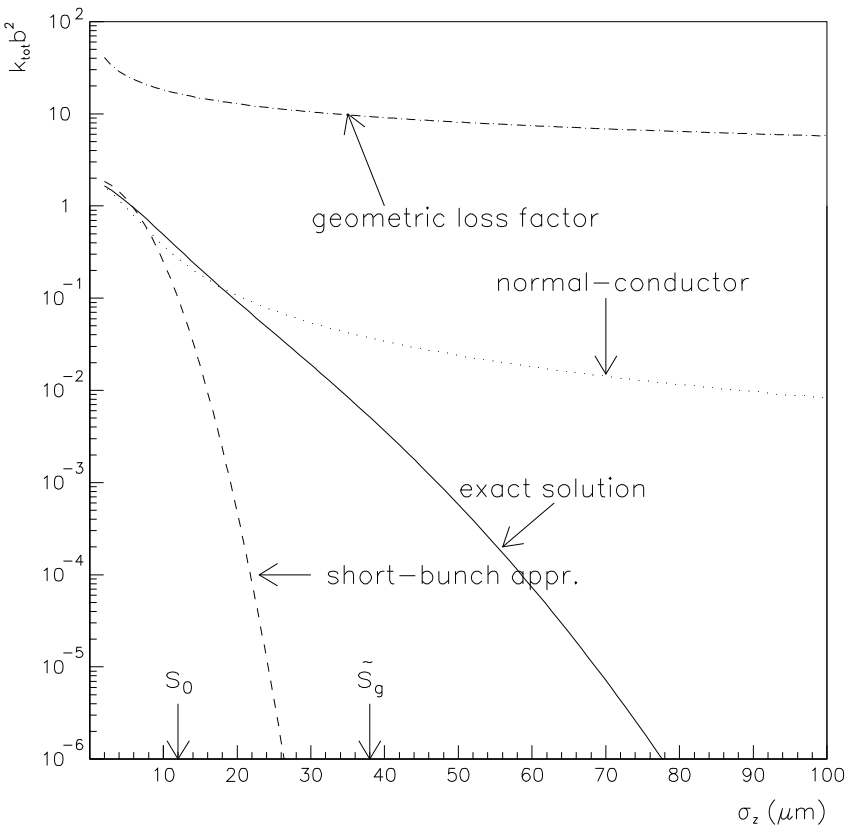

Figure 5: Loss factor $b^2 k_{tot}$ as a function of bunch length σ_z, for a superconducting niobium beam pipe at 2 K. Solid lines: numerical integration of Eq. (13); dashed line: short-bunch approximation, Eq. (21); dotted line: loss factor for normal-conducting niobium. dash-dotted line: geometric loss factor per unit length for a cavity of length $g = 115.4$ mm.

material	niobium (at 2–3 K)		copper (at room temp.)	
normal conductivity σ_n	3×10^{19} s^{-1}		5.8×10^{17} s^{-1}	
beam-pipe radius b	3 cm	5 mm	3 cm	5 mm
resistive length s_0	12 μm	3.4 μm	29 μm	8.8 μm
superconducting length $\tilde{s}_g$	38 μm		NA	
thermal conductivity $k(T)$	0.2 W cm^{-1} K^{-1}		4.0 W cm^{-1} K^{-1}	
density ρ	8.6 g cm^{-3}		9.0 g cm^{-3}	
specific heat c_p	10^{-4} J g^{-1} K^{-1} (s.c.)		0.39 J g^{-1} K^{-1}	

Table 1: Some parameters for a niobium or copper beam pipe and two different beam-pipe radii.